

# Nutrient levels and trade-offs control diversity in a model seasonal ecosystem

Amir Erez,<sup>1,\*</sup> Jaime G. Lopez,<sup>2,\*</sup> Benjamin Weiner,<sup>2</sup> Yigal Meir,<sup>3</sup> and Ned S. Wingreen<sup>1,2,†</sup>

<sup>1</sup>*Department of Molecular Biology, Princeton University, Princeton, New Jersey 08544, USA*

<sup>2</sup>*Lewis-Sigler Institute for Integrative Genomics, Princeton University, Princeton, New Jersey 08544, USA*

<sup>3</sup>*Department of Physics, Ben Gurion University of the Negev, Beer Sheva, Israel*

Microbial communities feature an immense diversity of species. Moreover, the extent of diversity correlates with outcomes ranging from ecosystem stability to favorable medical prognoses. Yet the mechanisms underlying microbial diversity are not well understood. Simple resource-competition models do not allow for a large number of distinct organisms, permitting coexistence of only as many species as resources. However, it was recently shown that metabolic trade-offs can lead to unlimited diversity in a steady-state chemostat model. Do such trade-offs permit diversity under more realistic, intermittent conditions of nutrient supply? Here, we demonstrate that in serial dilution culture, metabolic trade-offs allow for arbitrarily high diversity. Surprisingly, we find that, unlike the chemostat case, diversity depends on the amount of nutrient supplied to the community. The form of this dependence, however, varies with the precision of metabolic trade-offs and the presence of cross-feeding, immigration, or evolution. The large variation seen in this simple model suggests that real ecosystems may not obey a single universal relationship between nutrient supply and diversity.

Keywords: Microbial diversity | Resource-competition model | Serial dilution | Competitive exclusion

Microbial communities feature an immense diversity of organisms, with the typical human gut microbiota containing hundreds, and a gram of soil containing thousands, of distinct microbial genomes [1, 2]. These observations clash with a prediction of resource-competition models, known as the competitive-exclusion principle – namely, that steady-state coexistence is possible for only as many species as resources [3, 4]. This conundrum is familiarly known as the “paradox of the plankton” [5]. Solving this paradox may provide one key to predicting and controlling outcomes ranging from ecosystem stability to successful cancer treatments in humans [6–9]. Many possible solutions of the paradox have been offered: (i) the addition of interactions between microbes, such as cross-feeding or antibiotic production and degradation [10, 11], (ii) spatial heterogeneity [12], (iii) persistent non-steady-state dynamics [5]. While possible explanations for the paradox commonly invoke a steady supply of resources [13], in nature nutrients are rarely supplied in a constant and continuous fashion. In particular, seasonal variation is ubiquitous in ecology, influencing systems ranging from oceanic phytoplankton communities [14] to the microbiota of some human populations [15]. How does a variable nutrient supply influence diversity?

To address this question, we consider a known resource-competition model that permits high diversity at steady state due to metabolic trade-offs, but now in the context of serial dilution to reflect a more realistic variable nutrient supply. Serial dilution is well-established as an experimental approach. For example, the bacterial populations in the Lenski long-term evolution experiment [16], experiments on community assembly [17], and

antibiotic cross-protection [18] were all performed in serial dilution. While previous models of serial dilution have characterized competition between small numbers of species with trade-offs in their growth characteristics [19, 20], the theoretical understanding of diversity in serial dilution is much less developed than for chemostat-based steady-state growth.

Here, we show that metabolic trade-offs allow a serial dilution system to support unlimited coexistence, but that, unlike the chemostat case, community diversity depends upon both nutrient bolus and inoculum size. This dependence allowed us to explore an unresolved question in ecology [21–23]: what is the relationship between the amount of nutrient supplied and the resulting diversity of the community? Experimental studies of this question have mainly been performed in macroecological contexts [24–26], though recently there has been increased focus on microbial systems [27, 28]. In microbial experiments, some evidence has supported the “hump-shaped” unimodal trend predicted by many theories [29]. However, a meta-analysis by Smith [30] found no consistent trend across microbial experiments. What we observe here is concordant with Smith’s result: even in our highly simplified model, there is no general relationship between nutrient supply and diversity. Among the factors we find that influence this relationship are cross-feeding, relative enzyme budgets, and the presence of mutation. That so much variation appears in a simple model suggests that real ecosystems are not likely to display a single universal relationship between nutrient supply and diversity.

## Results

We employ the serial dilution model depicted in Fig. 1A. At the beginning of each batch ( $t = 0$ ), an inocu-

\*These authors contributed equally, listed alphabetically

†Electronic address: wingreen@princeton.edu

lum is specified as a collection of species  $\{\sigma\}$  with initial biomass densities  $\rho_\sigma(0)$  such that the total cellular inoculum biomass density is  $\rho_0 = \sum_\sigma \rho_\sigma(0)$ . Together with the inoculum, we supply a mixture of  $p$  nutrients each with concentration  $c_i(0)$ ,  $i = 1, \dots, p$  such that the total nutrient bolus concentration is  $c_0 = \sum_{i=1}^p c_i(0)$ . For simplicity, we assume ideal nutrient to biomass conversion, so that for a species to grow one unit of biomass density, it consumes one unit of nutrient concentration (this can be viewed as a choice of the nutrient units). During each batch, the species biomass densities  $\rho_\sigma(t)$  increase with time, starting at  $t = 0$ , and growth continues until the nutrients are fully depleted,  $\sum_{i=1}^p c_i(\infty) \approx 0$ . Thus, at the end of a batch, the total biomass density of cells is  $\sum_\sigma \rho_\sigma(\infty) = \rho_0 + c_0$ . The next batch is then inoculated with a biomass density  $\rho_0$  with a composition that reflects the relative abundance of each species in the total biomass at the end of the previous batch. This process is repeated until “steady state” is reached, i.e. when the biomass composition at the beginning of each batch stops changing.

In the model, a species  $\sigma$  is defined by its unique enzyme strategy  $\vec{\alpha}_\sigma = (\alpha_{\sigma,1}, \dots, \alpha_{\sigma,p})$  which determines its ability to consume different nutrients. Each species can consume multiple nutrients simultaneously, in line with the behavior of microbes at low nutrient concentrations [31]. Specifically, we assume that species  $\sigma$  consumes nutrient  $i$  at a rate  $j_{\sigma,i}$  (per unit biomass) that depends on nutrient availability  $c_i$  and on its enzyme allocation strategy  $\alpha_{\sigma,i}$  according to

$$j_{\sigma,i} = \frac{c_i}{K_i + c_i} \alpha_{\sigma,i}. \quad (1)$$

For simplicity, we take all Monod constants to be equal,  $K_i = K$  (a more general form of the nutrient model is considered in *SI Appendix* Sec. 4). During each batch, the dynamics of nutrient concentrations and biomass densities then follow from the rates  $j_{\sigma,i}$  at which the species consume nutrients:

$$\frac{dc_i}{dt} = - \sum_\sigma \rho_\sigma j_{\sigma,i}, \quad (2)$$

$$\frac{d\rho_\sigma}{dt} = \rho_\sigma \sum_i j_{\sigma,i}. \quad (3)$$

Since the level of one enzyme inevitably comes at the expense of another, we model this trade-off via an approximately fixed total enzyme budget  $E$ . Formally, we take  $\sum_i \alpha_{\sigma,i} = E + \varepsilon \xi_\sigma$ , where  $\xi_\sigma$  is a zero-mean and unit-variance Gaussian variable. Without loss of generality we take  $E = 1$ ; initially we set  $\varepsilon = 0$ . This allows us to visualize the strategies  $\vec{\alpha}_\sigma$  as points on a simplex, depicted as colored circles embedded in: (i) the interval  $[0, 1]$  for two nutrients (Fig. 1B), or (ii) a triangle for three nutrients (Fig. 1C). One can plot the nutrient bolus composition  $c_i/c_0$  on the same simplex, as depicted by the black diamonds in Fig. 1B and C. In what follows,

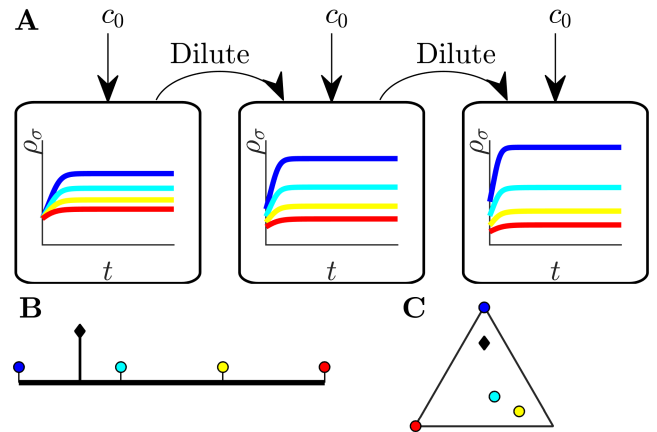


FIG. 1: Illustration of serial dilution resource-competition model. (A) Serial dilution protocol. Each cycle of batch growth begins with a cellular biomass density  $\rho_0$  and total nutrient concentration  $c_0$ . The system evolves according to Eqs. 2-3 until nutrients are completely consumed. A sample of the total biomass is then used to inoculate the next batch again at density  $\rho_0$ . (B) Representation of particular enzyme-allocation strategies  $\{\alpha_\sigma\}$  (colored circles) and nutrient supply composition  $c_i/c_0$  (black diamond) on a 2-nutrient simplex, where the right endpoint corresponds to 100% Nutrient 1. (C) Representation of particular strategies (circles) and nutrient supply (black diamond) on a 3-nutrient simplex.

we focus on the case of two nutrients, though the main results extend to an arbitrarily large number of nutrients.

One can intuit that our serial dilution model at very low nutrient bolus size will mimic a chemostat. Adding a small nutrient bolus, letting it be consumed, then removing the additional biomass, and repeating is tantamount to operating a chemostat with a fixed nutrient supply and dilution rate. Indeed, the limit  $c_0 \ll K$  yields the same steady state as a chemostat (*SI Appendix* Sec. 6). Thus, our results for serial dilution include and generalize those obtained for a closely related chemostat model [32]. Critically, it was shown there that in the presence of metabolic trade-offs, the chemostat can support a higher species diversity than prescribed by the competitive exclusion principle. Specifically, if the nutrient supply lies within the convex hull of the strategies on the simplex (visualized by stretching a rubber band around the outermost strategies), an arbitrarily large number of species can coexist at steady state. Thus, in the chemostat-limit of the cases shown in Figs. 1B and C all the species will coexist. Conversely, if the supply lies outside the convex hull, (e.g., if we swapped the positions of the left-most species and the supply in Fig. 1B) the number of surviving species would be strictly less than the number of nutrients, consistent with competitive exclusion. To understand the convex-hull rule, note that a state of arbitrarily high coexistence can only occur if the chemostat self-organizes to a “neutral” state in which the nutrient concentrations are all equal, and thus all strategies have the same growth rate. This state is achieved if and only if

the total enzyme abundances lie along the same vector as the nutrient supply, which is achievable only if the supply lies within the convex hull of the strategies present.

### Effect of Total Nutrient Bolus on Coexistence

In the chemostat limit, increasing the nutrient supply rate simply proportionally increases the steady-state population abundances. However, away from this limit we find that the magnitude of the nutrient bolus can qualitatively affect the steady-state outcome of serial dilutions. To understand this effect, we first consider a simple case of two nutrients and two species as depicted in Fig. 2A. The two species will coexist if each species is invulnerable to the other. In our example, we first determine the invulnerability of species R (strategy indicated by red circle) by species with strategies lying to its left. To this end, we choose a nutrient supply and perform model serial dilutions until steady state is reached. For a particular finite bolus size, we find that for all supplies within the hatched region an infinitesimal inoculum of any species lying to the left of R will increase more than R during a batch, and therefore can invade R. Similarly, we determine the invulnerability of species B (strategy indicated by blue circle) by any species with a strategy lying to its right, and find the second hatched region. The intersection of these hatched regions for which (1) B can invade R and (2) R can invade B is the supply interval of mutual invulnerability where these two species will stably coexist. The coexistence interval is bounded by the red and blue triangles, and each of these coexistence boundaries is a unique property of its corresponding species. We call these species-specific boundaries *remapped* because they generally lie at different locations on the simplex than the strategies they originated from, with the extent of remapping depending on the nutrient bolus size. (At a more technical level, the remapped boundary for a given species and bolus size is the nutrient supply for which, over the course of a batch, all nutrients are equally valuable).

Since the remapped coexistence boundaries depend on the nutrient bolus size  $c_0$ , changing bolus size can qualitatively change the steady-state outcome of serial dilutions. Figure 2B-D depicts an example of how  $c_0$  affects remapping, and the consequences for species coexistence. At low bolus size,  $c_0 \ll K$ , corresponding to the chemostat limit, Fig. 2B (left) shows that all species present achieve steady-state coexistence. This follows because the nutrient supply (black diamond) lies inside the convex hull. When  $c_0$  is increased to  $c_0 \approx K$  (Fig. 2C), the coexistence boundaries are remapped towards the center of the simplex (dashed arrow). In this example, the nutrient supply now lies outside the convex hull. This results in one winner species (the dark blue one nearest the supply), with all others decreasing exponentially from batch to batch. Strikingly, however, as bolus size is further increased to  $c_0 \gg K$ , the coexistence bound-

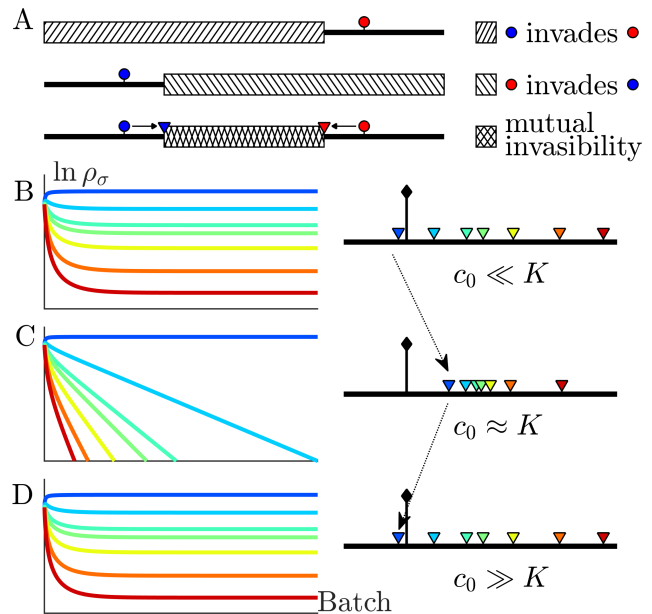


FIG. 2: The nutrient bolus size  $c_0$  affects the relative abundance of species and even their coexistence at steady state. (A) Schematic of the mutual invulnerability condition for two species and two nutrients. Top: The red species can be invaded by any species with a strategy to its left if the supply lies in the region marked by the hatched rectangle. Middle: Similarly, showing the supplies for which blue can be invaded by any species with a strategy to its right. Bottom: The intersection defines a mutual invulnerability region of supplies for which the two species red and blue will coexist. Triangles mark the boundaries of this coexistence region. (B-D) Example of the effect of  $c_0$  on coexistence for more than two species: the approach to steady state, showing  $\ln \rho_\sigma$  versus batch number (left column) with the corresponding  $c_0$ -dependent remapping of coexistence boundaries (right column). (B) For the chemostat limit  $c_0 \ll K$ , where  $K$  is the Michaelis constant for nutrient uptake, the triangles marking coexistence boundaries coincide with the species' strategies,  $\alpha_\sigma$ . (C) For  $c_0 \approx K$  the triangles are remapped towards the center of the simplex compared to the strategies  $\{\alpha_\sigma\}$ . In this example the nutrient supply (black diamond) ends up outside the coexistence boundaries, so only one species survives. (D) For  $c_0 \gg K$  the triangles again coincide with the strategies  $\{\alpha_\sigma\}$ , leading again to coexistence.

aries are remapped back to their original positions, so that the nutrient supply once again lies within the convex hull, and so steady-state coexistence of all species is recovered.

Why does the coexistence boundary of a species map back to its original strategy in the limit of large bolus size,  $c_0 \gg K$ ? In this limit, the nutrient uptake functions in Eq. 1 will be saturated during almost the entire period of a batch. Each species will therefore consume nutrients strictly in proportion to its strategy  $\alpha_{\sigma,i}$ . For the case of two nutrients (e.g., as shown in Fig. 1B), if there is only a single species present then if the supply lies anywhere to the left of its strategy, there will be some of Nutrient

2 remaining after Nutrient 1 has been consumed. Thus a single species can be invaded by any strategy to its left, provided the supply also lies to its left. Similarly, a species can be invaded by any strategy to its right if the supply lies to its right. This is exactly the condition for the coexistence boundary of a species to coincide with its actual strategy (details in *SI Appendix* Sec. 7).

We have rationalized coexistence in our serial dilution model in terms of mutual invasibility, but have not explicitly stated the condition for an arbitrary number of species to coexist in steady state. In the chemostat limit, all species coexist when the concentrations of all nutrients are equal, implying the same growth rate for all strategies. However, for serial dilutions the nutrient concentrations are generally not equal and are not even constant in time. Instead, it is the integrated growth contribution of every nutrient that must be equal to allow for arbitrary coexistence. In the case of equal enzyme budgets ( $\varepsilon = 0$ ), this condition occurs when the time integrals of the nutrient Monod functions within a batch are all equal, i.e.,

$$I_i = \int_0^\infty \frac{c_i}{K_i + c_i} dt = \text{const.} \quad (4)$$

To understand this condition for coexistence, note that the instantaneous rate of growth of a species  $\sigma$  is  $\sum_i \alpha_{\sigma,i} c_i / (K_i + c_i)$ , so that the fold increase of a species during a batch is  $\exp(\vec{\alpha}_\sigma \cdot \vec{I})$ . This fold increase will be equal for all species if and only if Eq. 4 holds. When there are two nutrients, Eq. 4 holds at steady state whenever the supply is inside the convex hull of the coexistence boundaries of the species present (details in *SI Appendix* Sec. 5). For more nutrients, the corresponding condition is that the region of coexistence is bounded by contours that connect the outermost remapped nodes.

### Steady-state Diversity

As is apparent in Fig. 2C, not all strategies are remapped to the same extent. In Fig. 3A, we plot the remapping of coexistence boundaries as a function of nutrient bolus  $c_0$ . Note that: (i) the specialists (0,1) and (1,0) and the perfect generalist (0.5,0.5) are not remapped at all; (ii) remapping is maximal for  $c_0 \approx K$ ; (iii) there is no remapping in both the  $c_0 \rightarrow 0$  and  $c_0 \rightarrow \infty$  limits (see also *SI Appendix* Fig. S1). The extent of remapping also depends on the inoculum size  $\rho_0$  as shown in Fig. 3B, which demonstrates that remapping is maximal for  $\rho_0 \ll K$  and vanishes for  $\rho_0 \gg K$ .

How does remapping influence steady-state species diversity? A useful summary statistic for quantifying diversity [33] is the effective number of species  $m_e = \exp[-\sum_\sigma P_\sigma \ln P_\sigma]$  where  $P_\sigma = \rho_\sigma(0)/\rho_0$ . Diversity as measured by  $m_e$  is shown in Fig. 3C for six choices of nutrient bolus composition. Notably, if the two nutrients are supplied equally (top curve, magenta),  $m_e$  is independent of  $c_0$  and coincides with the maximal possible diver-

sity (dashed black line), namely equal steady-state abundances of all species (Fig. 3D, top). Conversely, if Nutrient 1 comprises only 5% of supplied nutrient (Fig. 3C, bottom curve, cyan), the number of effective species  $m_e$  is lower than maximal even in the chemostat-limit of small bolus sizes  $c_0 \ll K$  and drops even further for  $c_0 \approx K$ . This loss of diversity is due to the dramatically lowered steady-state abundances of strategies that favor Nutrient 1 (Fig. 3D, bottom). For very large bolus sizes, diversity returns to its chemostat-limit, as expected from the lack of remapping for  $c_0 \gg K$ . Though here we focused on the case of two nutrients, these results extend to more nutrients. (For three nutrients see *SI Appendix* Fig. S9, S10).

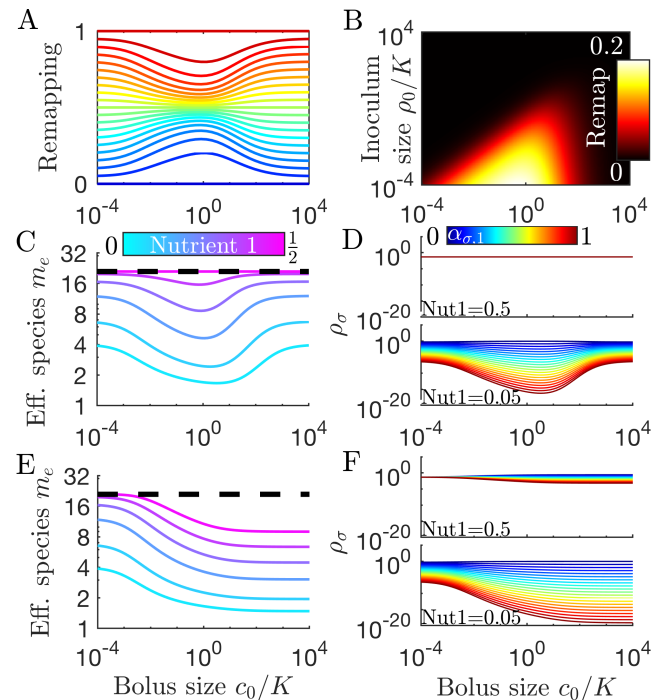


FIG. 3: Remapping of strategies at finite nutrient supply generally reduces species diversity. (A) As shown for the case of two nutrients, the remapping of strategies (i.e., the shift of coexistence boundaries) is non-monotonic with nutrient bolus size  $c_0$  (colors indicate 21 equally spaced strategies). (B) Heat map of the extent of remapping for strategy (0.2, 0.8) as a function of nutrient bolus size  $c_0/K$  and inoculum size  $\rho_0/K$ . (C) Steady-state effective number of species  $m_e$  as a function of bolus size  $c_0/K$  with equal initial inocula adding up to  $\rho_0/K = 10^{-3}$ ; the same initial conditions apply for panels D-F. Colors correspond to different nutrient supply compositions  $c_1/(c_1 + c_2)$ . Dashed black line: maximum diversity (equal species abundances) is attained when nutrient composition is (0.5, 0.5). (D) Steady-state species abundances  $\{\rho_\sigma\}$  for nutrient composition (0.5, 0.5) (top) and (0.05, 0.95) (bottom). (E, F) Same as C, D but with two trophic layers with Nutrient 1 a byproduct of metabolizing Nutrient 2: (E) effective number of species  $m_e$  and (F) species abundances  $\rho_\sigma$ .

### Cross-feeding

It is possible to extend Eqs. 2 and 3 beyond a single trophic layer, allowing for consumption of metabolic byproducts. This is a form of cross-feeding, which has generally been found to promote diversity [10] and stable community structure [17]. Here, cross-feeding is introduced through the byproduct matrix  $\Gamma_{i,i'}^\sigma$ , which converts the consumption of nutrient  $i'$  to production of nutrient  $i$  such that,

$$\frac{dc_i}{dt} = - \sum_{\sigma} \rho_{\sigma} \left( j_{\sigma,i} - \sum_{i'} \Gamma_{i,i'}^{\sigma} j_{\sigma,i'} \right). \quad (5)$$

We focus on the simplest case: initially supplying only Nutrient 2, with Nutrient 1 solely derived as a metabolic byproduct via  $\Gamma_{i,i'}^{\sigma} = \begin{pmatrix} 0 & \Gamma \\ 0 & 0 \end{pmatrix}$  for all species. When  $\Gamma = 1$ , upon consumption Nutrient 2 is perfectly converted to Nutrient 1, leading to an equal total supply of the two nutrients. More generally,  $\int_0^{\infty} \sum_{\sigma} \rho_{\sigma} j_{\sigma,1} dt = \Gamma c_2(0)$  which allows a direct comparison between the unitrophic and bitrophic regimes: starting with  $c_2(0)$  nutrient results in  $(\Gamma + 1)c_2(0)$  total nutrient, and hence the Nutrient 1 fraction is  $\frac{\Gamma}{\Gamma + 1}$  of the total.

How does cross-feeding influence diversity in our serial dilution model? In Fig. 3E we compare bitrophic diversity for six values of  $\Gamma$  to their unitrophic equivalents (in Fig. 3C). We note that: (i) bitrophy still supports diversity greater than the competitive-exclusion limit; (ii) in the chemostat regime,  $c_0 \ll K$ , the unitrophic and bitrophic schemes have identical values of  $m_e$ , and these drop as  $c_0 \rightarrow K$ ; (iii) but for bitrophy the  $m_e$  does not recover for  $c_0 \gg K$ ; (iv) even when the total supply of both nutrients is equal ( $\Gamma = 1$ ), bitrophy leads to lower than maximal  $m_e$  outside the chemostat limit. These features are clarified in Fig. 3F, which shows steady-state species abundances for  $\Gamma$  values leading to a total Nutrient 1 supply fraction of 0.5 and 0.05, and highlights the lower diversity for bitrophy compared to unitrophy for large nutrient bolus size. This difference is due to an "early-bird" effect: a species consuming supplied nutrient early in the batch can build a sizable population before the competing species that rely on its byproduct. The early-bird population then outcompetes the others for byproduct consumption. As such, this effect increases with  $c_0/\rho_0$ ; the effect also becomes stronger at low  $c_0/K$ , since this allows the early-bird species more time to grow more before the byproduct accumulates to high enough levels to be significantly consumed (Fig. S2).

### Population Bottlenecks

So far we have considered deterministic dynamics, which is appropriate for large populations. In natural settings, however, there are often small semi-isolated communities. For these communities, fluctuations can play

an important role. In particular, population bottlenecks can lead to large demographic changes [34]. How does the nutrient supply affect diversity in such communities? To address this question, we applied discrete sampling of a finite population when diluting from one batch to the next (see *SI Appendix Methods*). With this protocol, an "extinction" occurs when sampling yields zero individuals of a species. For a long enough series of dilutions such extinctions would ultimately lead to near-complete loss of diversity. For small real-world populations, however, diversity may be maintained by migration. To model such migration we augmented the population at each dilution with a "spike-in" from a global pool of species, in the spirit of MacArthur's theory of island biogeography [35].

In Fig. 4A we show results of spike-in serial dilutions for a population bottleneck of 1000 cells. 95% of these cells are sampled from the previous batch, while 5% are sampled from a global pool, with equal abundances of 21 equally spaced strategies (*cf.* Fig. 3A). The resulting  $m_e$  vs.  $c_0$  curves have maximal  $m_e$  for all six nutrient fractions in the regime  $c_0 \ll K$  where the 5% spike-in dominates sampling noise. As expected, for a balanced nutrient supply at any  $c_0$ , all species have the same average abundance (Fig. 4B top). By contrast, when Nutrient 1's fraction is low (Fig. 4A cyan and 4B bottom), increasing  $c_0$  increases the abundance gaps between the species, reflecting the uneven competition for Nutrient 2. Overall, the spike-in protocol leads to higher diversity at low  $c_0$  than the deterministic case (starting from equal species abundances but with no spike-in, Fig. 3C). For large  $c_0$ , the  $m_e$  vs.  $c_0$  curves for these two protocols are indistinguishable. The only noticeable difference is that the spike-in maintains a higher level of the least competitive strains, but since these abundances are still low, this difference is not reflected in the  $m_e$  values.

### Unequal enzyme budgets

While we have assumed exact trade-offs to achieve diversity within a resource-competition model, the trade-offs present among real microorganisms will not be exact. For the serial dilution protocol with spike-ins, diversity is maintained by migration and so it is possible to relax the constraint of exact trade-offs. How does diversity depend on the nutrient supply if we allow species to have different enzyme budgets? We implemented random differences in species enzyme budgets by setting  $\varepsilon = 0.1$ , i.e. a standard deviation of 10%, and plotted effective number of species  $m_e$  in Fig. 4C. As in the  $\varepsilon = 0$  limit (Fig. 4A), at sufficiently small  $c_0$  the spike-in procedure dominates both sampling noise and differential growth rates due to unequal enzyme budgets. Raising  $c_0$  leads to a drop in  $m_e$  (albeit still above the competitive-exclusion limit). Examining the species abundances in Fig. 4D, we note that differences in enzyme budget establish a fitness hierarchy even when nutrient fractions are equal (top), with

those species with the highest budgets increasing in relative abundance as  $c_0$  increases. The asterisk (\*) marks the species with the highest total enzyme budget, which becomes the most abundant for  $c_0 > K$ . Reducing Nutrient 1’s fraction to 0.05 results in a shifting abundance hierarchy (Fig. 4D, bottom): at low  $c_0$  the highest abundance species is the one that consumes only Nutrient 2, as in the equivalent  $\varepsilon = 0$  case. However, increasing  $c_0$  results in increased abundance for the species with the highest enzyme budget – which would ultimately lead to its domination for sufficiently large  $c_0$ . In short, for spike-in serial dilutions the influence of unequal enzyme budgets depends on the nutrient supply, such that the species with the largest budgets dominate for large, unbiased supplies.

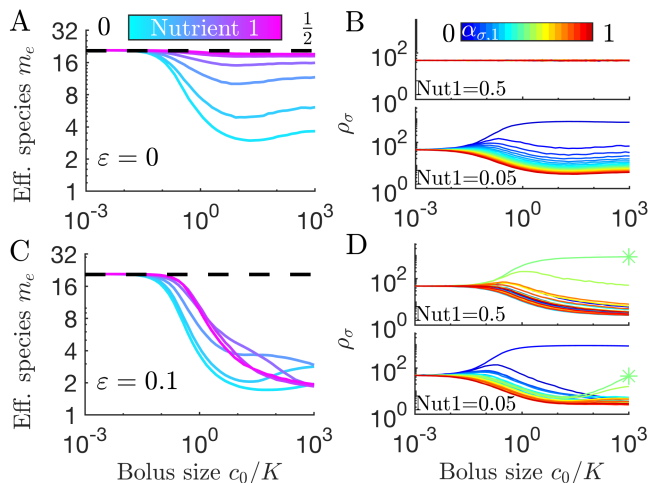


FIG. 4: Diversity of small communities with migration. Each batch was inoculated with 1000 cells: 950 cells sampled without replacement from the previous batch, 50 cells sampled from 21 equally abundant, equally spaced strategies. (A) Effective number of species  $m_e$  for different compositions of two nutrients (colors) as a function of nutrient bolus size  $c_0/K$ . (B) Average steady-state species abundances  $\{\rho_\sigma\}$  for nutrient composition (0.5, 0.5) (top) and (0.05, 0.95) (bottom). (C) as A, but with random species-specific total enzyme budget specified by  $\varepsilon = 0.1$ . (D) as B but with species-specific enzyme budgets from C. Asterisk (\*) indicates the species with the largest enzyme budget.

### Mutation-Selection Balance

So far, we have considered experimental serial dilution systems as a proxy for the variable nutrient supply of natural ecosystems. To more closely capture the dynamic equilibrium of populations in the wild, we extend our model to include mutation-selection balance. Specifically, we introduce mutations as random changes in metabolic strategy [36]. Since a mutant is initially present as a single cell, it becomes essential to stochastically model the population dynamics, including both

reproduction and sampling for each inoculum. Within a batch, instead of the deterministic ODEs of Eqs. 2-3 we simulate stochastic dynamics using Gillespie’s method [37], summarized in Table 2 in *SI Appendix Methods*. For large populations, the resulting steady state matches the deterministic one, including the remapping observed in Fig. 3A (see *SI Appendix Fig. S3*). To account for mutations, we modify the growth term to allow for *mutation*, whereby when species  $\sigma$  grows by one cell, instead of making another  $\sigma$ , it makes a  $\sigma'$  cell, i.e.  $\sigma \rightarrow \sigma + \sigma'$ . *Mutation* occurs at a rate  $\nu \rho_\sigma \sum_i j_{\sigma,i}$ , while normal growth,  $\sigma \rightarrow 2\sigma$ , occurs at a rate  $(1 - \nu) \rho_\sigma \sum_i j_{\sigma,i}$ . Together, stochastic reproduction, inter-batch sampling, and intra-batch mutations lead to complex dynamics whereby a species can appear, flourish for a number of batches, then die out, with different species replacing it. This results in fluctuations in the number of species present from batch to batch (*SI Appendix Fig. S4*).

How does species diversity depend on nutrient bolus size  $c_0$  under conditions of mutation-selection balance? Previously, we saw that diversity decreased for  $c_0 \approx K$  due to the remapping of coexistence boundaries. Now with mutations, the larger the nutrient bolus  $c_0$ , the more mutations within a batch, leading to more species at the end of the batch (*SI Appendix Fig. S5, S6*). How do these opposing tendencies combine? Figure 5A shows the effective number of species,  $m_e$ . As  $c_0$  increases, the decrease in  $m_e$  due to remapping is offset by mutations generating new species. As a result, for these parameters,  $m_e$  is flat as  $c_0 \approx K$ . As  $c_0$  increases further,  $m_e$  does increase, due to both mutations and reduced remapping. This is evident in Fig. 5B which shows more species and flatter rank-abundance curves for higher  $c_0$  for a balanced nutrient supply (magenta). Even for an unbalanced nutrient supply (cyan), diversity increases for large enough  $c_0/K$ . (Lower values of  $c_0/K$  are shown in *SI Appendix Figs. S7, S8*). Broadly speaking, mutations in our model lead to a “rich get poorer” effect in which high-abundance species feed low-abundance species with a steady stream of mutants, leading to higher overall species diversity.

### Discussion

Natural ecosystems experience variations in the timing and magnitude of nutrient supply, and the impact of these variations on species diversity is not fully understood [20, 30]. To explore the impact of variable nutrient supply, we modeled resource competition in a serial dilution framework and analyzed the model’s steady states. We found that variable nutrient supply still allows for the high diversity seen in the continuous supply (“chemostat”) version of the model. Surprisingly, introducing variable nutrient supply also led to a dependence of diversity on the amount of supplied nutrients.

Finding a general relation between the amount of nutrient supplied to a community and its diversity is a long-standing goal of theoretical ecology [21–23]. We found

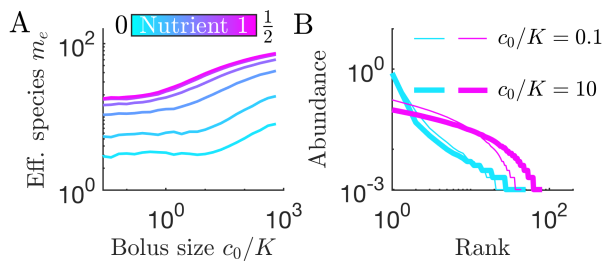


FIG. 5: Diversity of species under mutation-selection balance. Starting from an inoculum of 1000 cells, a fraction  $\nu = 0.01$  of cell divisions results in a mutation to a randomly-selected one of 201 evenly spaced strategies. Populations recorded at the start of each batch. (A) Effective number of species  $m_e$  for different nutrient compositions (colors) as a function of nutrient bolus size  $c_0/K$ . (B) Rank-abundance curves for Nutrient 1 fractions 0.05 (cyan) and 0.5 (magenta); line thickness indicates value of  $c_0/K$ .

that in our model, the form of the nutrient-diversity relation (NDR) can change based on model details. The model has two regimes: a low diversity and a high diversity regime. The former satisfies competitive exclusion (no more species than resources) whereas the latter exceeds competitive exclusion and occurs when the nutrient supply lies within the convex hull of the metabolic strategies present [32]. In the high diversity regime, the NDR can take several forms. For a single trophic layer and multiple supplied nutrients, the model has a U-shaped NDR. For a single supplied nutrient with cross-feeding via a second trophic layer, the NDR is monotonically decreasing. Finally, allowing daughter cells to have different strate-

gies than their parents (“mutation”) leads to a monotonically *increasing* NDR. Thus, even in this very simple model there is no general NDR. Experimental studies have reached similar conclusions, reporting both decreasing [27] and increasing [28] NDRs. A meta-analysis found examples of both monotonic and non-monotonic NDRs, with no single form dominating [30]. Our theoretical results, together with these experimental findings, indicate that there may be no single universal NDR. While we have focused on microbial systems, this conclusion is consistent with results from recent work in plants [26].

Our modeling predictions, e.g. the convex hull condition and the high diversity resulting from “spike-in” even when enzyme budgets are unequal, are in principle testable. There are two key assumptions in our model: (i) that an organism consumes multiple nutrients simultaneously; (ii) that an organism has fixed metabolic enzyme levels independent of nutrient composition. Both of these assumptions are supported by experiments on glucose and galactose uptake in *E. coli* at low nutrient levels [31, 38]. Indeed, *E. coli* appears to possess an approximate  $\bar{\alpha} = (0.5, 0.5)$  strategy on glucose and galactose. If this ratio can be modulated, one could test key theoretical predictions via competitions among *E. coli* strains.

#### Acknowledgments

This work was supported by National Institutes of Health (www.nih.gov) Grant R01 GM082938 (A.E., Y.M., and N.S.W), and National Science Foundation Grant GRFP DGE-1656466 (J.G.L.).

- 
- [1] Daniel R (2005) The metagenomics of soil. *Nature Reviews Microbiology* 3(6):470–478.
- [2] Meisel JS, Grice EA (2016) The Human Microbiome. *Genomic and Precision Medicine: Foundations, Translation, and Implementation: Third Edition* pp. 63–77.
- [3] Levin SA (1970) Community Equilibria and Stability, and an Extension of the Competitive Exclusion Principle. *Am. Nat.* 104(939):413–423.
- [4] Armstrong RA, McGehee R (1980) Competitive Exclusion. *Am. Nat.* 115(2):151–170.
- [5] Hutchinson GE (1961) The paradox of the plankton. *Am. Nat.* 95(882):137–145.
- [6] Ptacnik R, et al. (2008) Diversity predicts stability and resource use efficiency in natural phytoplankton communities. *Proc. Natl. Acad. Sci. U.S.A.* 105(13):5134–5138.
- [7] van Elsland JD, et al. (2012) Microbial diversity determines the invasion of soil by a bacterial pathogen. *Proc. Natl. Acad. Sci. U.S.A.* 109(4):1159–1164.
- [8] Taur Y, et al. (2014) The effects of intestinal tract bacterial diversity on mortality following allogeneic hematopoietic stem cell transplantation. *Blood* 124(7):1174–1182.
- [9] Stein RR, et al. (2013) Ecological modeling from time-series inference: Insight into dynamics and stability of intestinal microbiota. *PLOS Computational Biology* 9(12):e1003388.
- [10] Goyal A, Maslov S (2018) Diversity, Stability, and Reproducibility in Stochastically Assembled Microbial Ecosystems. *Physical Review Letters* 120(15):158102.
- [11] Kelsic ED, Zhao J, Vetsigian K, Kishony R (2015) Counteraction of antibiotic production and degradation stabilizes microbial communities. *Nature* 521(7553):516–519.
- [12] Huisman J, van Oostveen P, Weissing FJ (1999) Species Dynamics in Phytoplankton Blooms: Incomplete Mixing and Competition for Light. *Am. Nat.* 154(1):46–68.
- [13] Palmer MW (1994) Variation in species richness: Towards a unification of hypotheses. *Folia Geobotanica et Phytotaxonomica* 29(4):511–530.
- [14] Chang FH, Zeldis J, Gall M, Hall J (2003) Seasonal and spatial variation of phytoplankton assemblages, biomass and cell size from spring to summer across the north-eastern New Zealand continental shelf. *Journal of Plankton Research* 25(7):737–758.
- [15] Smits SA, et al. (2017) Seasonal cycling in the gut microbiome of the hadza hunter-gatherers of tanzania. *Science* 357(6353):802–806.
- [16] Lenski R, Travisano M (1994) Dynamics of Adaptation and Diversification. *Proc. Natl. Acad. Sci. U.S.A.*

- 91(July):6808–6814.
- [17] Goldford JE, et al. (2018) Emergent simplicity in microbial community assembly. *Science* 361(6401):469.
- [18] Yurtsev EA, Conwill A, Gore J (2016) Oscillatory dynamics in a bacterial cross-protection mutualism. *Proc. Natl. Acad. Sci. U.S.A.* 113(22):6236–6241.
- [19] Stewart FM, Levin BR (1973) Partitioning of Resources and the Outcome of Interspecific Competition : A Model and Some General Considerations. *Am. Nat.* 107(954):171–198.
- [20] Smith HL (2011) Bacterial competition in serial transfer culture. *Math. Biosci.* 229(2):149–159.
- [21] Tilman D (1982) *Resource Competition and Community Structure*. (Princeton U. Press).
- [22] Abrams PA (1995) Monotonic or Unimodal Diversity-Productivity Gradients: What Does Competition Theory Predict. *Ecology* 76(7):2019–2027.
- [23] Leibold MA (1996) A graphical Model of Keystone Predators in Food Webs: Trophic Regulation of Abundance, Incidence, and Diversity Patterns in Communities. *Am. Nat.* 147(5):784–812.
- [24] Mittelbach GG, et al. (2001) What Is the Observed Relationship Between Species Richness and Productivity? *Ecological Monographs* 82(9):2381–2396.
- [25] Waide RB, Willig MR, Steiner CF (1999) The relationship between productivity and species richness. *Annual Review of Ecology and Systematics* 30:257–300.
- [26] Adler PB, et al. (2011) Productivity Is a Poor Predictor of Plant Species Richness. *Science* 1750(September):1750–1754.
- [27] Bienhold C, Boetius A, Ramette A (2011) The energy-diversity relationship of complex bacterial communities in arctic deep-sea sediments. *The ISME Journal* 6:724.
- [28] Bernstein HC, et al. (2016) Trade-offs between microbiome diversity and productivity in a stratified microbial mat. *The ISME Journal* 11:405.
- [29] Kassen R, Buckling A, Bell G, Ralney PB (2000) Diversity peaks at intermediate productivity in a laboratory microcosm. *Nature* 406(6795):508–512.
- [30] Smith VH (2007) Microbial diversity-productivity relationships in aquatic ecosystems. *FEMS Microbiology Ecology* 62(2):181–186.
- [31] Kovarova-Kovar K, Egli T (1998) Growth Kinetics of Suspended Microbial Cells: From Single-Substrate-Controlled Growth to Mixed-Substrate Kinetics. *Microbiol. Mol. Biol. Rev.* 62(3):646–666.
- [32] Posfai A, Tallefumier T, Wingreen NS (2017) Metabolic Trade-Offs Promote Diversity in a Model Ecosystem. *Physical Review Letters* 118(2):1–5.
- [33] Jost L (2006) Entropy and diversity. *Oikos* 113(2):363–375.
- [34] Abel S, Abel zur Wiesch P, Davis BM, Waldor MK (2015) Analysis of bottlenecks in experimental models of infection. *PLOS Pathogens* 11(6):e1004823.
- [35] MacArthur RH, Wilson EO (2001) *The theory of island biogeography*. (Princeton U. Press).
- [36] Good BH, Martis S, Hallatschek O (2018) Adaptation limits ecological diversification and promotes ecological tinkering during the competition for substitutable resources. *Proc Natl Acad Sci USA* 115(44):E10407.
- [37] Gillespie DT (1977) Exact stochastic simulation of coupled chemical reactions. *J. Phys. Chem.* 81(25):2340–2361.
- [38] Lendenmann U, Snozzi M, Egli T (1996) Kinetics of the simultaneous utilization of sugar mixtures by *Escherichia coli* in continuous culture. *Appl. Environ. Microbiol.* 62(5):1493–1499.